

Highlights

Primary-Auxiliary Model Scheduling Based Estimation of the Vertical Wheel Force in a Full Vehicle System

Xueke Zheng, Runze Cai, Shuixin Xiao, Yu Qiu, Jun Zhang, Mian Li

- A modeling scheduling framework for sensor-to-sensor identification problems for the purpose of signal estimation is proposed.
- The method is applicable to the systems with switching linear dynamics.
- An experimental validation on a full vehicle system is performed to reconstruct the vertical wheel force.
- Good accordance between the measurements and the estimates is achieved with the reasonable accuracy level under multiple working conditions.

Primary-Auxiliary Model Scheduling Based Estimation of the Vertical Wheel Force in a Full Vehicle System

Xueke Zheng^a, Runze Cai^{a,b,*}, Shuixin Xiao^a, Yu Qiu^c, Jun Zhang^{a,d}, Mian Li^{a,d}

^a*University of Michigan – Shanghai Jiao Tong University Joint Institute, Shanghai Jiao Tong University, 800 Road, Minghang district, Shanghai, 200240, China*

^b*School of Mechanical Engineering, Shanghai Jiao Tong University, 800 Road, Minghang district, Shanghai, 200240, China*

^c*SAIC Motor Corporation Limited, 201 Anyan Road, Jiading district, Shanghai, 201800, China*

^d*Department of Automation, Shanghai Jiao Tong University, 800 Road, Minghang district, Shanghai, 200240, China*

Abstract

In this work we study estimation problems in nonlinear mechanical systems subject to non-stationary and unknown excitation, which are common and critical problems in design and health management of mechanical systems.

A primary-auxiliary model scheduling procedure based on time-domain transmissibilities is proposed and performed under switching linear dynamics: In addition to constructing a primary transmissibility family from the pseudo-inputs to the output during the offline stage, an auxiliary transmissibility family is constructed by further decomposing the pseudo-input vector into two parts. The auxiliary family enables to determine the unknown working condition at which the system is currently running at, and then an appropriate transmissibility from the primary transmissibility family for estimating the unknown output can be selected during the online estimation stage. Moreover, Finite Impulse Response (FIR) models, ridge regression, and Bayes classifiers are applied to realize the model scheduling procedure. As a result, the proposed approach offers a generalizable and explainable solution to the signal estimation problems in nonlinear mechanical systems in the context of switching linear dynamics with unknown inputs.

A numerical example and a real-world application to the estimation of the vertical wheel force in a full vehicle system are, respectively, conducted to demonstrate the effectiveness of the proposed method. During the vehicle design phase, the vertical wheel force is the most important one among Wheel Center Loads (WCLs), and it is often measured directly with expensive, intrusive, and hard-to-install measurement devices during full vehicle testing campaigns. Meanwhile, the estimation problem of the vertical wheel force has not been solved well and is still of great interest. The experimental results show good performances of the proposed method in the sense of estimation accuracy for estimating the vertical wheel force.

Keywords: Primary-auxiliary model scheduling, Transmissibility, Vertical wheel force, Wheel center loads, Automotive durability engineering

1. Introduction

When designing a new vehicle, the durability performances can be assessed by considering the knowledge of Wheel Center Loads (WCLs), i.e., longitudinal, lateral, and vertical wheel forces,

*Corresponding author.

Email address: cairunze@sjtu.edu.cn (Runze Cai)

camber, torque, and steer moments, as input quantities [1]. In the current practice, the WCLs are measured directly by so-called Wheel Force Transducers (WFTs) during Road Load Data Acquisition (RLDA) testing campaigns in which prototype vehicles are driven on proving grounds or public roads. However, WFTs are expensive, intrusive, and time-consuming to install. Particularly, it is economically infeasible to install WFTs in each vehicle when multiple vehicles need to be tested [2, 3]. Therefore, in order to facilitate the vehicle design phase, it is appealing to resort to alternative ways of obtaining WCLs without directly measuring them by WFTs.

1.1. Physically Based and Data-driven Methods

The vehicle dynamic system is a complex and nonlinear mechanical system [2–4]. In order to accurately estimate WCLs by some other easy-to-measure quantities, E. Risaliti et al. [3, 4] develop an approach based on multi-body simulation models and augmented Extended Kalman Filters (EKFs). The multi-body based approach achieves a good performance in a McPherson suspension system in 4 experimental runs. However, the approach may have three disadvantages: First, the highly accurate multi-body simulation model is not easy to obtain in some cases [2]; Second, the model parameters of EKFs are difficult to determine when prototype vehicles are driven under a variety of working conditions on proving grounds or public roads (in which cases the excitation of the system is unknown and non-stationary); Finally, the use of EKFs might be problematic when the system is strongly nonlinear [3]. Nevertheless, the main advantage of using multi-body based approach is to gain more physical insights on the effects of the variation of the system parameters [2].

An alternative is to use data-driven models instead of multi-body simulation models to build the input-output relations between WCLs and other measurements such as the strain gauges, suspension deflections and accelerations. Several common data-driven models such as linear Auto-Regressive with eXtra input (ARX), Polynomial Nonlinear State Space (PNLSS), and the Recurrent Neural Network (RNN) models are used to estimate WCLs. However, it turns out that the linear ARX models cannot capture the nonlinear effects, and PNLSS as well as RNN models lack the generalization ability [2]. In addition, the computational cost and memory requirements are challenging factors for real-time systems when the nonlinear models are involved. As a result, the estimation problem of WCLs in RLDA testing campaigns has not been solved well and is of great interest, hence a simple and effective method is in high demand.

It is worthwhile to notice that the vertical wheel force not only is the most important load among WCLs, but also is most affected by the variation of model parameters in multi-body model based method [3]. Therefore, a successful estimation of the vertical wheel force is a good step for the estimation of WCLs.

1.2. Sensor-to-Sensor and Piece-Wise Affine (PWA) System Identification

Sensor-to-sensor system identification problems have received considerable research interests in recent past [5–10]. In this type of problems, the relation between the response of a subset of sensors and the response of the remaining ones is modeled in the frequency domain or in the time domain [5, 9, 11–13], and such type of modeling is extensively required by the applications of structural modeling and structure health monitoring systems [14–17]. In this area, it is often assumed that the system is linear [8, 9, 18], and transmissibilities are introduced to model the relation between the signals from sensors without knowing the excitation of the system, which

can be non-stationary. Moreover, due to good properties such as Bounded-Input Bounded-Output (BIBO) stability, Finite Impulse Response (FIR) models have proven to be better candidates over ARX models for estimating transmissibilities in many sensor-to-sensor identification problems [6, 19, 20]. However, FIR models are also linear and thus directly applying them to the nonlinear mechanical systems will lead to poor performances (which are also shown in our experimental results in Section 5).

Recent years have witnessed a growing interest on Piece-Wise Affine (PWA) system identification methods which have proven to be effective for problems involving complex nonlinear systems with large data sets [21, 22]. Many literatures focus on studying piecewise ARX models for the purpose of system control [21, 22]. However, when it comes to classifying the regressor domain of piecewise FIR models for the purpose of signal estimation, data classification should be carefully addressed since the dimension of the regressor domain is often much higher.

1.3. The Proposed Method: Primary-Auxiliary Model Scheduling Procedure

In this work, we consider the situation that the data of the vertical wheel force and some other easy-to-measure quantities (e.g., accelerations and suspension deflections) obtained by affordable and common sensors is collected from multiple working conditions on proving grounds, and our goal is to use these easy-to-measure quantities to estimate the vertical wheel force in a full test vehicle.

We validate that a full vehicle dynamic system can be approximated by a switching linear dynamic system [23] with unknown inputs, and each sub-system describes the dynamics of the system running at an unknown working condition. Note that determining the unknown working conditions during the online estimation stage is the bottleneck in the estimation of the vertical wheel force.

The response of easy-to-measure quantities is essentially the outputs of the true system in the sensor-to-sensor system identification context. Based on this observation, besides constructing a primary time-domain transmissibility family from the response of easy-to-measure quantities to the vertical wheel force under multiple working conditions during the offline stage, another auxiliary time-domain transmissibility family is constructed by decomposing these easy-to-measure quantities into two parts. The auxiliary transmissibility family is further used for constructing the Bayes classifier which determines the unknown working conditions during the online estimation stage, and then an appropriate transmissibility from the primary transmissibility family is selected for estimating the unknown vertical wheel force.

1.4. Main Contributions and Paper Outline

The main contribution of this paper includes: We propose a primary-auxiliary model scheduling procedure for signal estimation in nonlinear mechanical systems subject to non-stationary and unknown excitation, which can be approximated by switching linear systems with unknown inputs. The key reason behind the success of the proposed method is the strategic construction of the auxiliary transmissibility family which enables model scheduling during the online estimation stage. Thus, the unknown working conditions are determined in a sensible manner. The benefits of introducing the auxiliary transmissibility family are

- The construction of FIR models and the Bayes classifier is computationally tractable; no nonlinear or nonconvex optimizations are involved.

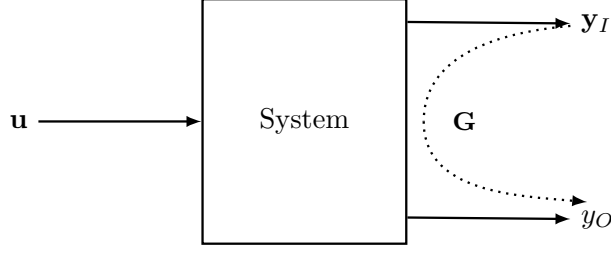


Figure 1: The transmissibility from pseudo-inputs \mathbf{y}_I to output y_O .

- The transmissibility family allows to avoid classifying the high dimensional regressor, which could lead to poor performances in PWA system identification methods.

For the reason above, the proposed method offers a generalizable and explainable solution to the signal estimation problems in nonlinear mechanical systems in the context of switching linear dynamics with unknown inputs.

A real experiment representing an industrial application (i.e., the estimation of the vertical wheel force in RLDA testing campaigns) as a particular case is used to validate the proposed methodology. In comparison with limited experimental runs carried out with a suspension system in work [2–4], the experimental runs are carried out under a variety of working conditions (covering the typical ones in RLDA testing campaigns as many as possible) with a full vehicle system in this work, which leads to more realistic experimental settings for RLDA testing campaigns. Since the six WCLs can be estimated independently within the framework of the primary-auxiliary model scheduling, the estimation of the vertical wheel force can be extended to the estimation of the other five WCLs.

The rest of the paper is organized as follows: In Section 2, we briefly introduce FIR models, Maximum Likelihood Estimation (MLE), and ridge regression. In Section 3, a primary-auxiliary model scheduling procedure during the online estimation stage is detailed. In Section 4, a numerical example of a quarter-car suspension system is shown, and a real-world application to the vertical wheel force estimation in a full vehicle system is demonstrated for the effectiveness of the proposed method in Section 5. Finally, conclusion remarks and future works are presented in Section 6.

2. Linear Regression for FIR Models

Consider a dynamical system as shown in Fig. 1, where \mathbf{u} denotes the excitation or the inputs to the system, and \mathbf{y}_I as well as y_O are the outputs of the system. In this section, we assume that the system is linear, and the relation from \mathbf{y}_I to y_O can be described as a discrete-time transmissibility, denoted by \mathbf{G} , which will be used later in the nonlinear system context in Section 3.

2.1. Maximum Likelihood Estimation (MLE) of FIR Model Parameters

Now consider the following Multiple-Input Single-Output (MISO) model for \mathbf{G} given by

$$y_O(t) = \mathbf{b}_0^T \mathbf{y}_I(t) + \dots + \mathbf{b}_n^T \mathbf{y}_I(t - n) + \epsilon(t), \quad (1)$$

where $\mathbf{y}_I(t) \in \mathbb{R}^{n_I}$ and $y_O(t) \in \mathbb{R}$ are, respectively, noise-free pseudo-inputs and output measurements of transmissibilities, n_I is the dimension of the pseudo-inputs, $\mathbf{b}_i \in \mathbb{R}^{n_I}$ are parameters, $i = 0, \dots, n$, and $\epsilon(t)$ is the residual representing the unmodeled dynamics. We intend to identify

the parameters \mathbf{b}_i 's given \mathbf{y}_I and y_O over a period of time, say, $t = n + 1, \dots, N + n$. Now it is easily verified that Eq. (1) can be reformulated as a linear regression problem

$$y_O(t) = \phi_I^T(t)\theta + \epsilon(t), \quad t = n + 1, \dots, N + n, \quad (2)$$

where $\theta = [\mathbf{b}_0^T \cdots \mathbf{b}_n^T]^T$, and we assume that $\epsilon(t)$ is an i.i.d. Gaussian random variable for all t , and the regressor $\phi_I(t) = [\mathbf{y}_I^T(t) \cdots \mathbf{y}_I^T(t - n)]^T$. Rewriting Eq. (1) by stacking the elements (rows) $\mathbf{y}(t)$ and $\phi_I^T(t)$ in the vectors (matrices) yields the vector form of the regression problem as

$$\mathbf{Y}_O = \Phi_I \theta + \mathbf{E}, \quad (3)$$

where

$$\mathbf{Y}_O = \begin{bmatrix} y_O(n+1) \\ \vdots \\ y_O(N+n) \end{bmatrix}, \Phi_I = \begin{bmatrix} \phi_I^T(n+1) \\ \vdots \\ \phi_I^T(N+n) \end{bmatrix}, \mathbf{E} = \begin{bmatrix} \epsilon(n+1) \\ \vdots \\ \epsilon(N+n) \end{bmatrix}. \quad (4)$$

A statistical argument for estimating θ in Eq. (3) is that the measurement \mathbf{Y}_O can be regarded as a realization of a random variable with a normal distribution

$$\mathbf{Y}_O \sim \mathcal{N}(\Phi_I \theta, \sigma^2 \mathbf{I}), \quad (5)$$

where σ^2 is noise variance of $\epsilon(t)$, and \mathbf{I} is an identity matrix of the appropriate dimension. By solving the optimization problem

$$\underset{\theta}{\text{minimize}} \quad \|\mathbf{Y}_O - \Phi_I \theta\|_2^2, \quad (6)$$

the maximum likelihood estimator of θ is given by

$$\hat{\theta}^{\text{MLE}} = (\Phi_I^T \Phi_I)^{-1} \Phi_I^T \mathbf{Y}_O, \quad (7)$$

provided that $\Phi_I^T \Phi_I$ is non-singular, which is guaranteed if the pseudo-inputs \mathbf{y}_I is persistently exciting [24].

Remark 1. There are two reasons of modeling the relation between \mathbf{y}_I and y_O by an FIR structure:

- (i) An FIR model structure is Bounded-Input Bounded-Output (BIBO) stable even if the transfer function from the excitation to the pseudo-inputs is a non-minimum phase system, i.e., there are zeros outside of the unite circle in the discrete-time case, which indicates that the transmissibility is unstable. It is worth noting that the instability of the transmissibility induces noncausal components in the transmissibility impulse response [16], in which case a noncausal FIR model can be used to model the relation between the pseudo-inputs and the output with minor changes [20].
- (ii) An FIR model provides a consistent estimate of true parameters if the sequence $\{\mathbf{y}_I(t)\}$ is independent of the sequence $\{\epsilon(t)\}$. A detailed study on the consistency of least squares methods for modeling parameters in the presence of uncorrelated and correlated input, process, and output noise can be found in [25].

2.2. Ridge Regression of FIR Model Parameters

Sometimes occasions may arise when the pseudo-inputs are poorly exciting during the identification of FIR models. In such cases, one issue of the FIR model is the selection of the model order n which is usually unknown in advance. For the model parameter θ , an inappropriate selection of n can lead to either a large bias or variance. To strike a balance between the bias and variance, a successful method is ridge regression [26]. Applying ridge regression, the regression problem in Eq. (3) can be solved by considering the regularized least squares problem

$$\underset{\theta}{\text{minimize}} \quad \|\mathbf{Y}_O - \Phi_I \theta\|_2^2 + \rho \theta^T \theta, \quad (8)$$

where $\rho \theta^T \theta$ is a flexibility penalty term, and ρ is a tuning parameter [26]. The optimization problem (8) admits a closed-form solution

$$\hat{\theta}^{\text{ridge}} = (\Phi_I^T \Phi_I + \rho \mathbf{I})^{-1} \Phi_I^T \mathbf{Y}_O. \quad (9)$$

Furthermore, the variance σ^2 can be estimated as [27]

$$\hat{\sigma}^2 = \frac{\|\mathbf{Y}_O - \Phi_I \hat{\theta}^{\text{ridge}}\|_2^2}{N - n_I(n + 1)}. \quad (10)$$

The ridge regression problem in Eq. (8) is frequently used in statistics to overcome the issue of ill-conditioning in the original linear regression problem. The tuning parameter ρ is usually chosen by cross-validation or other nonlinear optimization methods [26, 28].

In this work we choose ρ in a simpler manner. Let λ_{\max} and λ_{\min} denote the largest and smallest eigenvalues of $\Phi_I^T \Phi_I$, respectively. In order to avoid the matrix $\Phi_I^T \Phi_I + \rho \mathbf{I}$ to be close to being singular, the condition number of $\Phi_I^T \Phi_I + \rho \mathbf{I}$, denoted by $\kappa(\Phi_I^T \Phi_I + \rho \mathbf{I})$, is controlled below a reasonable level denoted by C_{lim} , e.g., $C_{\text{lim}} = 1 \times 10^6$. It can be easily verified that the largest and smallest eigenvalues of the matrix $\Phi_I^T \Phi_I + \rho \mathbf{I}$ are given by $\lambda_{\max} + \rho$ and $\lambda_{\min} + \rho$, respectively. We set the condition number of the matrix $\Phi_I^T \Phi_I + \rho \mathbf{I}$ below C_{lim} , i.e.,

$$\kappa(\Phi_I^T \Phi_I + \rho \mathbf{I}) = \frac{\lambda_{\max} + \rho}{\lambda_{\min} + \rho} \leq C_{\text{lim}}. \quad (11)$$

It can be verified that the inequality (11) is satisfied if we choose ρ as

$$\rho = \begin{cases} 0, & \kappa(\Phi_I^T \Phi_I) \leq C_{\text{lim}}, \\ \frac{\lambda_{\max} - \lambda_{\min} \cdot C_{\text{lim}}}{C_{\text{lim}} - 1}, & \kappa(\Phi_I^T \Phi_I) > C_{\text{lim}}. \end{cases} \quad (12)$$

3. Primary-Auxiliary Model Scheduling for Signal Estimation

In this section, we consider the system in Fig. 1 in a nonlinear setting, and the primary-auxiliary model scheduling procedure is deployed based on FIR models.

3.1. Model Scheduling Based on Primary and Auxiliary Transmissibility Families

As mentioned previously, the performance of modeling the system by one single FIR model is possibly poor due to non-linearity issues. As is commonly described in PWA system identification

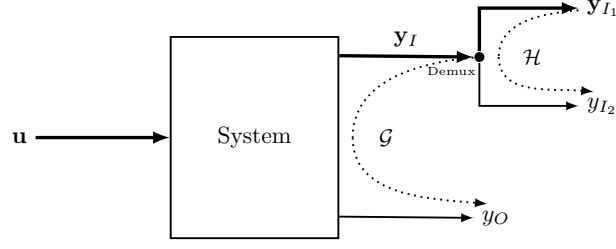


Figure 2: transmissibilities from \mathbf{y}_I to y_O , and \mathbf{y}_{I1} to y_{I2} .

problems [21], suppose the system can be approximately described by multiple transmissibilities, each of which provides a satisfactory description of the system under a different working condition \mathcal{C}_q , where $q \in \mathcal{Q} = \{1, \dots, Q\}$. Explicitly, the relation from \mathbf{y}_I to y_O can be represented by a transmissibility family $\mathcal{G} = \{\mathbf{G}_q \mid q \in \mathcal{Q}\}$, where \mathbf{G}_q 's can be approximately modeled by FIR models introduced in Section 2. Then the problem comes down to determining which working condition the system is currently at when estimating y_O . In sensor-to-sensor problems shown in Fig. 2, if the pseudo-inputs \mathbf{y}_I can be decomposed as

$$\mathbf{y}_I = \begin{bmatrix} \mathbf{y}_{I1} \\ y_{I2} \end{bmatrix}, \quad (13)$$

where $\mathbf{y}_{I1}(t) \in \mathbb{R}^{n_{I1}}$, $y_{I2}(t) \in \mathbb{R}$ for each t , whenever the dimension of \mathbf{y}_I is greater than one (which is the case here for \mathbf{G}), thus the relation from \mathbf{y}_{I1} to y_{I2} can be described by another transmissibility family $\mathcal{H} = \{\mathbf{H}_q \mid q \in \mathcal{Q}\}$ modeled by FIRs. The family \mathcal{H} enables us to connect FIR models with data classification in pattern recognition, where we aim to find a decision rule which assigns a class to each observation based on the system outputs [29].

The overall procedure proposed in this work is shown in Fig. 3, which consists of two stages: During the online stage, the pseudo-inputs \mathbf{y}_I is known and a Bayes classifier is used to choose the transmissibility \mathbf{H}_{q^*} from \mathcal{H} that best fits the working condition the system is currently at, and then a scheduler receives the index q^* and chooses the appropriate transmissibility \mathbf{G}_{q^*} from \mathcal{G} for calculating the unknown output y_O from the given \mathbf{y}_I . Note that \mathcal{H} for the Bayes classifier as well as \mathcal{G} for the scheduler are precalculated during the offline stage.

3.2. Offline Stage and Online Stage

In this subsection, we elaborate the procedure illustrated in Fig. 3:

- (i) During the offline stage, two families of transmissibilities \mathcal{H} and \mathcal{G} are constructed based on offline data sets from different working conditions $\mathcal{C}_1, \dots, \mathcal{C}_Q$;
- (ii) During the online stage, a Bayes classifier is constructed based on \mathcal{H} , and the appropriate transmissibility from \mathcal{G} is assigned to the online data.

Offline Stage. The transmissibility \mathbf{H}_q 's from \mathcal{H} is modeled by the FIR model as follows

$$y_{I2,q}(t) = \mathbf{b}_{0,q}^T \mathbf{y}_{I1,q}(t) + \dots + \mathbf{b}_{n,q}^T \mathbf{y}_{I1,q}(t - n) + \epsilon_{I,q}(t), \quad (14)$$

where $q = 1, \dots, Q$, the sequences $\{\mathbf{y}_{I,q}(t), y_{O,q}(t)\}$ denote the offline data set for q -th working condition, $\{\mathbf{b}_{0,q}, \dots, \mathbf{b}_{n,q}\}$ are parameters, and $\epsilon_{I,q}(t)$ is an i.i.d. Gaussian random variable with variance $\sigma_{I,q}^2$ given a period of time.

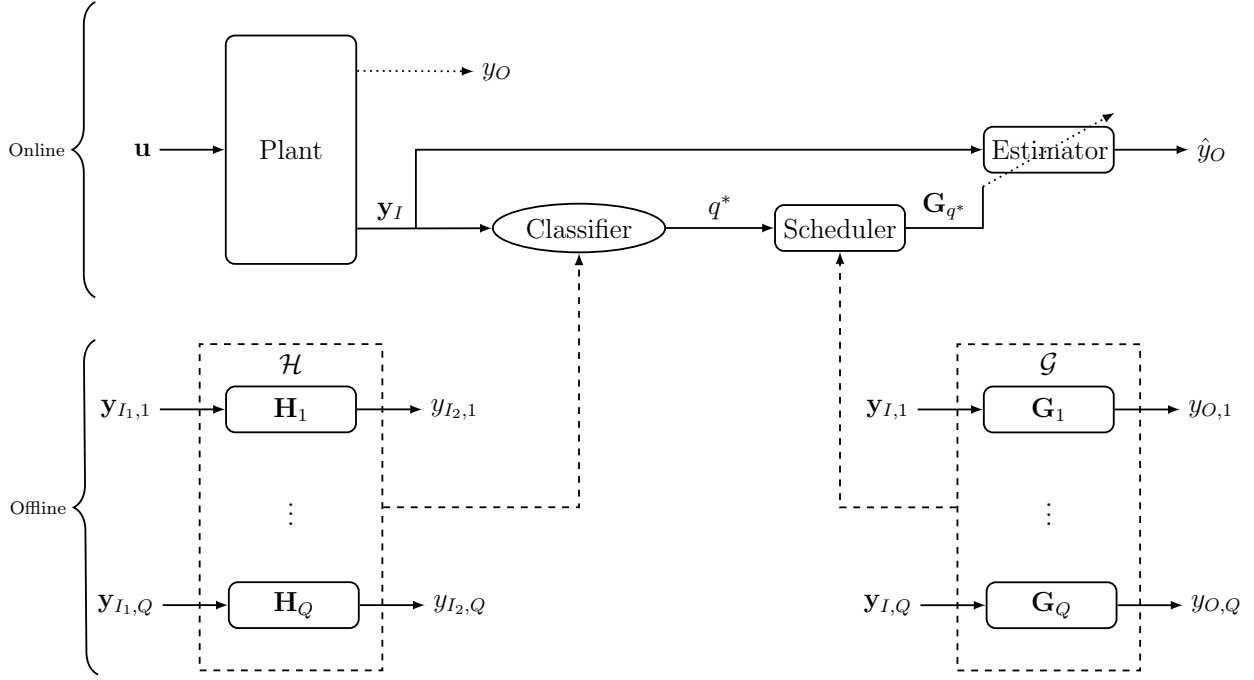


Figure 3: The overall procedure of the sensor-to-sensor system identification and primary-auxiliary model scheduling during offline and online stages, respectively.

Following Eq. (2), we rewrite Eq. (14) as follows

$$y_{I_2,q}(t) = \phi_{I_1,q}^T(t)\theta_{I,q} + \epsilon_{I,q}(t). \quad (15)$$

The estimates of $\theta_{I,q}$'s and $\sigma_{I,q}^2$'s can be obtained according to Eq. (9) and (10), respectively. Note that \mathbf{G}_q 's from \mathcal{G} can also be modeled in a similar manner.

Online Stage. When it comes to assigning the \mathbf{H}_{q^*} that best fits the sequences $\{y_{I_2}(t), \phi_{I_1}(t)\}$, where $t = n+1, \dots, N+n$, during online estimation, we assume the sequence is stationary, and denote $p(\mathbf{H}_q)$'s as the prior probabilities defined by users for assigning \mathbf{H}_q 's. Then, by Bayes formula, we have

$$p(\mathbf{H}_q | \mathbf{Y}_{I_2}) = \frac{p(\mathbf{Y}_{I_2} | \mathbf{H}_q)p(\mathbf{H}_q)}{p(\mathbf{Y}_{I_2})}, \quad (16)$$

where $p(\mathbf{H}_q | \mathbf{Y}_{I_2})$ is the posterior probability,

$$p(\mathbf{Y}_{I_2} | \mathbf{H}_q) = (2\pi\hat{\sigma}_{I,q}^2)^{-N/2} \exp\left[-\frac{1}{2\hat{\sigma}_{I,q}^2}(\mathbf{Y}_{I_2} - \Phi_{I_1}\hat{\theta}_{I,q})^2\right] \quad (17)$$

$$p(\mathbf{Y}_{I_2}) = \sum_{q=1}^Q p(\mathbf{Y}_{I_2} | \mathbf{H}_q)p(\mathbf{H}_q) \quad (18)$$

$$\mathbf{Y}_{I_2} = [y_{I_2}(n+1) \ \cdots \ y_{I_2}(N+n)]^T \quad (19)$$

$$\Phi_{I_1} = [\phi_{I_1}(n+1) \ \cdots \ \phi_{I_1}(N+n)]^T, \quad (20)$$

and $\hat{\theta}_{I,q}$ and $\hat{\sigma}_{I,q}^2$ are estimates of $\theta_{I,q}$ and $\sigma_{I,q}^2$ for \mathbf{H}_q , respectively. Furthermore, the best \mathbf{H}_{q^*} from \mathcal{H} is selected as follows

$$\mathbf{H}_{q^*} = \arg \max_{\mathbf{H}_q \in \mathcal{H}} p(\mathbf{H}_q \mid \mathbf{Y}_{I_2}) \quad (21)$$

$$= \arg \max_{\mathbf{H}_q \in \mathcal{H}} \log p(\mathbf{H}_q \mid \mathbf{Y}_{I_2}) \quad (22)$$

$$= \arg \max_{\mathbf{H}_q \in \mathcal{H}} L_q, \quad (23)$$

where

$$L_q = \log p(\mathbf{H}_q) - N \log \hat{\sigma}_{I,q} - \frac{1}{2\hat{\sigma}_{I,q}^2} \|\mathbf{Y}_{I_2} - \Phi_{I_1} \hat{\theta}_{I,q}\|_2^2. \quad (24)$$

Now according to Eq. (2) and Eq. (9), the estimated output $\hat{y}_O(t)$ can be calculated by

$$\hat{y}_O(t) = \phi_I^T(t) \hat{\theta}_{O,q^*}, \quad t = n+1, \dots, N+n, \quad (25)$$

where $\hat{\theta}_{O,q^*}$ is estimated parameter for \mathbf{G}_{q^*} obtained during the offline stage.

Remark 2. The choice of y_{I_2} follows two principles from physical insights:

1. The Signal-to-Noise Ratios (SNRs) should be sufficient when the system undergoes different working conditions;
2. The relation between \mathbf{y}_{I_1} and y_{I_2} has to be different under different offline working conditions $\mathcal{C}_1, \dots, \mathcal{C}_Q$.

Otherwise, L_q 's in Eq. (24) calculated by Q auxiliary transmissibilities could be quite close if the prior probabilities are equal, which leads to ineffectiveness of the Bayes classifier.

Given the primary-auxiliary model scheduling procedure above, we will see in the next sections that the auxiliary transmissibility family \mathcal{H} which is used for constructing the Bayes classifier is capable of assigning an appropriate transmissibility \mathbf{G}_{q^*} to the online data $\{\mathbf{y}_I(t)\}$.

4. Numerical Validation

In this section, we present a numerical example aimed at verifying the effectiveness of the proposed primary-auxiliary model scheduling procedure for signal estimation problems in switching linear dynamic systems with unknown inputs.

4.1. Demonstration of the Primary-Auxiliary Model Scheduling Procedure at Online Stage

Fig. 4 shows a quarter-car suspension system, where k_r is the tire stiffness, k_s and c_s are spring and damper coefficients, respectively. The input of the system is the displacement denoted by z_r , and the displacements of the sprung mass and unsprung mass are denoted by z_s and z_u , respectively. Then the state-space form of the quarter-car suspension system in continuous time can be represented by

$$\begin{aligned} \dot{x}(t) &= A_c x(t) + b_c z_r(t) \\ y(t) &= C x(t) + d z_r(t), \end{aligned} \quad (26)$$

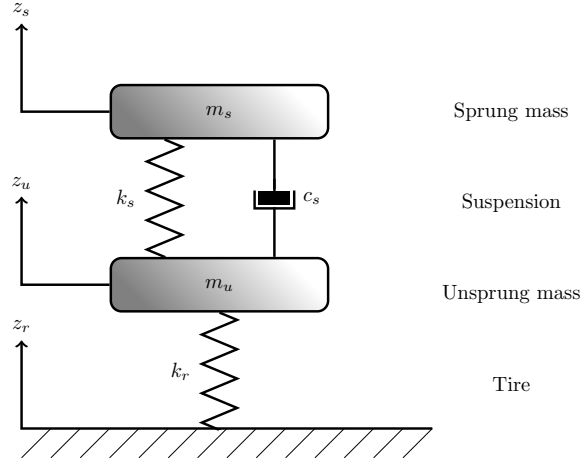


Figure 4: A simple quarter-car suspension system.

where $x(t) = [z_s(t) \dot{z}_s(t) z_u(t) \dot{z}_u(t)]^T$, $y(t) = [y_{I_1}(t) y_{I_2}(t) y_O(t)]^T$, and

$$A_c = \begin{bmatrix} 0 & 1 & 0 & 0 \\ -\frac{k_s}{m_s} & -\frac{c_s}{m_s} & \frac{k_s}{m_s} & \frac{c_s}{m_s} \\ 0 & 0 & 0 & 1 \\ \frac{k_s}{m_u} & \frac{c_s}{m_u} & -\frac{k_s+k_r}{m_u} & -\frac{c_s}{m_u} \end{bmatrix}, \quad b_c = \begin{bmatrix} 0 \\ 0 \\ 0 \\ \frac{k_r}{m_u} \end{bmatrix}, \quad (27)$$

$$C = \begin{bmatrix} \frac{k_s}{m_u} & \frac{c_s}{m_u} & -\frac{k_s+k_r}{m_u} & -\frac{c_s}{m_u} \\ -\frac{k_s}{m_s} & -\frac{c_s}{m_s} & \frac{k_s}{m_s} & \frac{c_s}{m_s} \\ 1 & 0 & -1 & 0 \end{bmatrix}, \quad d = \begin{bmatrix} \frac{k_r}{m_u} \\ 0 \\ 0 \end{bmatrix}. \quad (28)$$

We would like to estimate the relative displacement y_O between unsprung mass m_u and sprung mass m_s based on y_{I_1} (the acceleration of m_u) and y_{I_2} (the acceleration of m_s).

In practice, the physical parameters could be different when working conditions change. For sake of simplicity, we consider two working conditions \mathcal{C}_1 and \mathcal{C}_2 , and their physical parameters are listed in Tab. 1.

Table 1: The physical parameters of the quarter-car suspension system with two working conditions.

Parameters	Units	Numerical values	
		\mathcal{C}_1	\mathcal{C}_2
m_s	kg	300	300
m_u	kg	40	40
k_s	N m ⁻¹	2.0×10^4	4.0×10^4
k_r	N m ⁻¹	1.8×10^5	2.0×10^5
c_s	N s m ⁻¹	1.5×10^3	2.5×10^3

The system is discretized using a zero-order hold to obtain

$$\begin{aligned} x(t+1) &= Ax(t) + bz_r(t) \\ y(t) &= Cx(t) + dz_r(t) \end{aligned} \quad (29)$$

where $A = e^{A_c T}$, $b = A_c^{-1}(A - I)b_c$, and the sampling time T is 0.1 s. The input is a realization

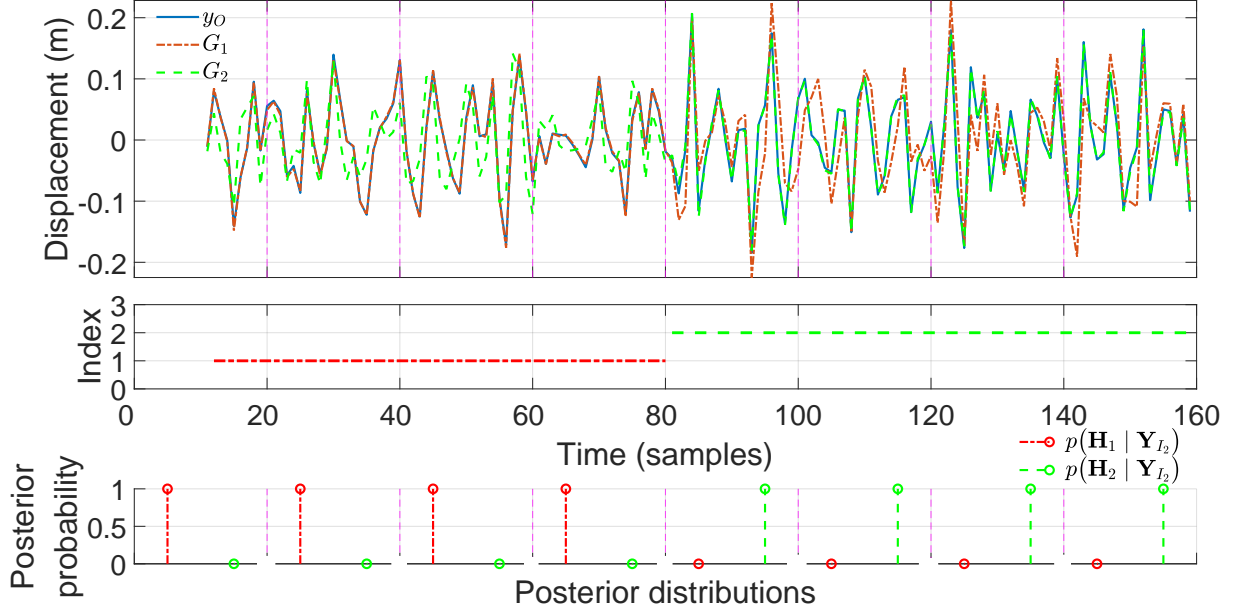


Figure 5: The illustration of the model scheduling procedure. Note that the validation data set is segmented into 8 sub-intervals, where the procedure is sequentially carried out. Top: the target output and its estimates by primary transmissibilities; Middle: evolution of transmissibilities; Bottom: the posterior distributions calculated by Eq. (16) in Section 3.2 for 8 sub-intervals.

of a zero-mean, white, Gaussian random process with 0.01 m^2 variance. FIR models with model order $n = 10$ are used to estimate model parameters of the primary and auxiliary transmissibility families. The ridge regression with $C_{\text{lim}} = 1 \times 10^6$ in Section 2.2 is applied to tackle ill-conditioning issues in the original linear regression. The measurements y_{I_1}, y_{I_2}, y_O are added by zero-mean white Gaussian noise with SNR values of 50. The prior distribution is $p(\mathbf{H}_1) = p(\mathbf{H}_2) = 0.5$.

The training data set contains 1000 data points. The validation data set contains 160 data points, which is segmented into 8 sub-intervals. Matlab function `lsim` is used for plotting simulated time responses of two sub-systems.

The evolution of switching linear dynamics is as follows: At the beginning, the switching system is running at working condition \mathcal{C}_1 at sample points 11–80. After 80 sample points, the system is switched to working condition \mathcal{C}_2 . Fig. 5 shows the illustration of the model scheduling procedure, where the estimation performance of y_O by primary transmissibilities, the evolution of primary transmissibilities, and posterior distributions of auxiliary transmissibilities calculated by Eq. (16) in Section 3.2 are presented, from which we can observe

- (i) The primary transmissibility G_1 can successfully estimate y_O at sample points 11–80. Correspondingly, the posterior probabilities $p(\mathbf{H}_1 | \mathbf{Y}_{I_2})$ at sub-intervals 1–4 are close to 1;
- (ii) The primary transmissibility G_2 can successfully estimate y_O at sample points 81–160. Correspondingly, the posterior probabilities $p(\mathbf{H}_2 | \mathbf{Y}_{I_2})$ at sub-intervals 5–8 are close to 1,

and it indicates that the evolution of primary transmissibilities coincide with the evolution of switching linear dynamics. Note that the transient effect at around data sample 80 is fast and can be negligible.

Thus, we can see in this numerical example that FIR models can approximate the transmissibilities very well and the Bayes classifier can successfully identify the working condition \mathcal{C}_q .

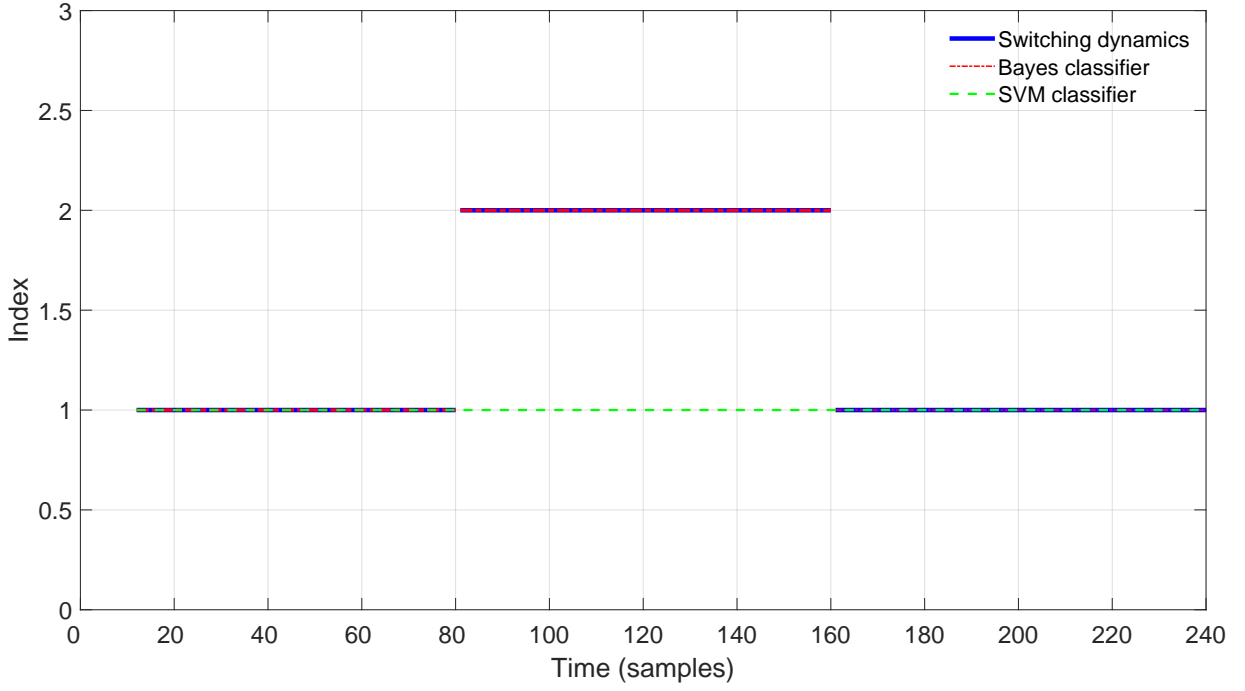


Figure 6: The evolution of the switching dynamics as well as the transmissibilities from \mathbf{y}_I to y_O according to the Bayes classifier and the SVM classifier. Note that the validation data set is segmented into 12 sub-intervals (i.e., 11–20, 21–40, ..., 221–240), where two classifiers are sequentially carried out.

4.2. A Comparative Study Between Bayes Classifiers and SVM Classifiers

Support Vector Machine (SVM) classifiers are often used for classifying the regressor $\phi_I(t)$ in Eq. (3) in PWA system identification methods [21, 22]. The decision rule of the SVM classifier is:

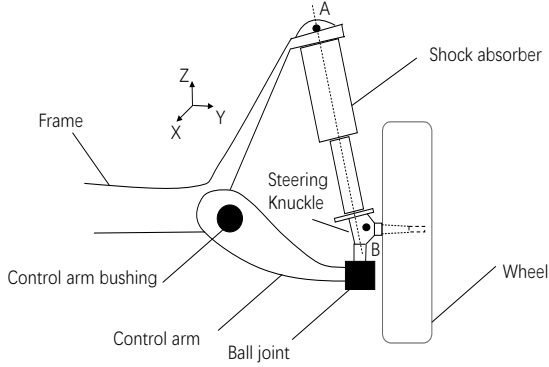
$$q^* = g(\phi_I(t)), \quad (30)$$

where $g(\phi_I(t))$ is a discriminant function which assigns the index q^* to the regressor $\phi_I(t)$. For a sequence $\{\phi_I(t), t = n + 1, \dots, n + N\}$, it is classified according to a majority vote among the discriminant functions $\{g(\phi_I(t)) \mid t = n + 1, \dots, n + N\}$. Matlab function `fitcecoc` (the hyperparameters are optimized as far as possible) is used to construct the SVM classifier, which is sequentially carried out in 12 sub-intervals, i.e., 11–20, 21–40, ..., 221–240, in validation data.

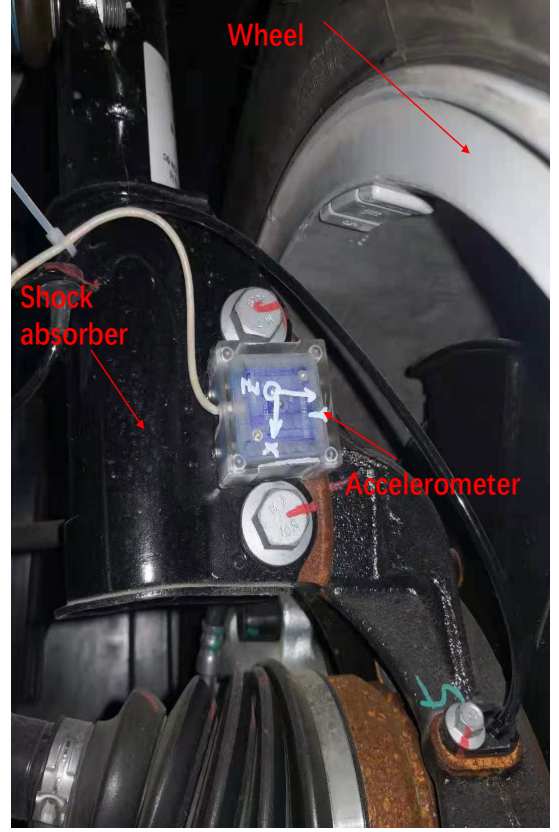
Fig. 6 shows the evolution of switching dynamics as well as the transmissibilities from \mathbf{y}_I to y_O according to the Bayes classifier and the SVM classifier. In this example, we can observe the evolution of the transmissibility obtained from the Bayes classifier coincides with the evolution of switching linear dynamics (at the beginning, the system is running at working condition \mathcal{C}_1 , after which it is switched to \mathcal{C}_2 , in the end it is switched back to \mathcal{C}_1), while the evolution of the transmissibility obtained from the SVM classifier deviates from the evolution of the dynamics when the system is switched to working condition \mathcal{C}_2 . It is not surprising that the Bayes classifier achieves the excellent classification accuracy, due to one-to-one correspondence between the auxiliary transmissibilities and the working conditions. It seems that the SVM classifier cannot extract the informative features, and thus fails to identify the working conditions. More discussions on the success of Bayes classifiers and the failure of SVM classifiers will be given in Remark 5 and Remark 6, respectively, along with the experimental results in Section 5.



(a) The wheel force transducer measuring WCLs is installed on the wheels.



(b) A sketch of a quarter-car suspension system.



(c) The accelerometer is installed close to the wheel center.

Figure 7: The locations of the accelerometers and the wheel force transducer.

5. Experimental Validation

In this section, we demonstrate the effectiveness of the proposed method by presenting a real-world industrial application to the vertical wheel force in a full vehicle system.

Fig. 7a shows the WFTs measuring WCLs (including the vertical wheel force) in a test vehicle. For the sake of clarity, Fig. 7b shows the locations of the sensors on a sketch of a quarter-car suspension system: Accelerations in the X, Y, Z directions at the position A, B as well as the suspension deflection are the known pseudo-inputs \mathbf{y}_I . The vertical wheel force is represented by y_O , which is the unknown output. Fig. 7c shows the accelerometer measuring accelerations at position B in the full test vehicle.

In the experimental runs on a proving ground, 58 working conditions (over 2×10^4 data samples with sampling frequency 512 Hz are collected at each working condition) are considered, and they can be roughly classified into four categories shown in Tab. 2. Note that these working conditions cover the typical ones in RLDA testing campaigns as many as possible. Fig. 8 shows four examples of road profiles. The data is preprocessed to be of mean zero.

5.1. Estimation performances Under Individual Working Conditions

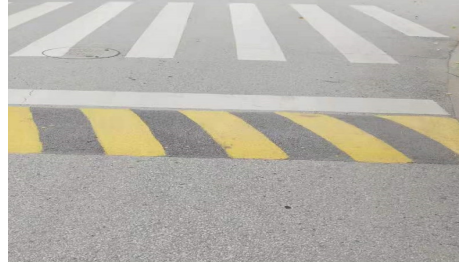
For a given working condition, the data set is split into two parts: the training data set and the validation data set. The training data set is used for constructing an FIR model from \mathbf{y}_I to y_O under the given working condition, and the validation data set is used for evaluating the performance of the constructed FIR model.

Table 2: Four categories of working conditions on a proving ground

Category	Description
1.	Driving straight on roads of random or periodic profiles such as Belgium block, smooth gravel, and washboard roads at various vehicle speeds.
2.	Driving over bumps, railway crosses, and potholes at various vehicle speeds.
3.	Steering at various vehicle speeds.
4.	Braking on roads of random or periodic profiles at slight, medium, and heavy levels.



(a) Belgium block road profile.



(b) Speed bump road profile.



(c) Pothole road profile.



(d) Smooth gravel road profile.

Figure 8: Four examples of road profiles.

The values of the following measure of fit are introduced [30, 31]

$$\text{FIT} = 100 \cdot \left(1 - \frac{\|\mathbf{Y}_O - \hat{\mathbf{Y}}_O\|_2}{\|\mathbf{Y}_O - \bar{\mathbf{Y}}_O\|_2} \right) \%, \quad (31)$$

where $\mathbf{Y}_O = [y_O(n+1) \cdots y_O(N+n)]^T$ are measurements collected from sensors, $\hat{\mathbf{Y}}_O$ is the estimate of \mathbf{Y}_O , and $\bar{\mathbf{Y}}_O$ is the mean of all entries of \mathbf{Y}_O . Eq. (31) indicates that the performance gets better as FIT gets closer to 100%.

Fig. 9 shows the estimation performances of the vertical force in validation data sets regarding to four working conditions (i.e., the test vehicle is driven on four types of road profiles shown in Fig. 8), one by one, and a zoom in the same result is shown in Fig. 10, from which we can observe that good accordance between the measurements and the estimates is achieved. Furthermore, we consider the 58 working conditions, and Tab. 3 shows the good estimation performances in the sense of FIT, which validates that the relation between responses of \mathbf{y}_{I_2} and y_{I_1} in the vehicle system can be approximated by an FIR model under a given working condition.

Next we will show the estimation performances of the proposed primary-auxiliary model scheduling procedure introduced in Section 3.

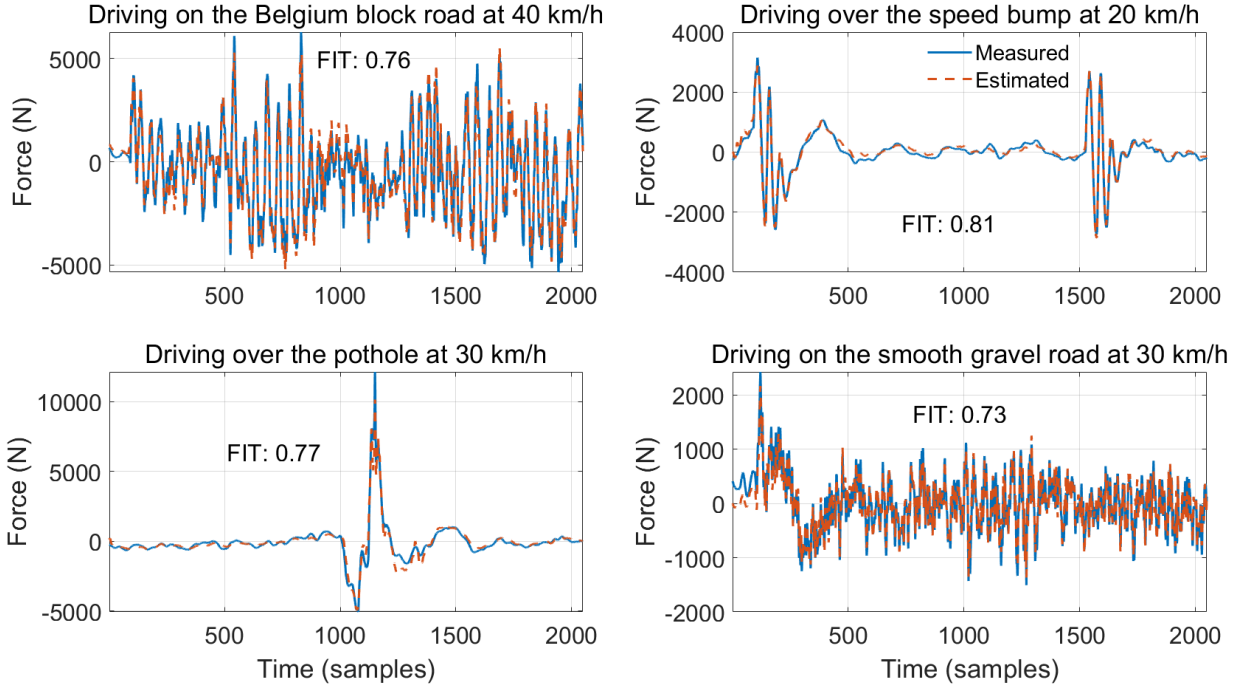


Figure 9: The measurements and estimates when the vehicle is driven on the four road profiles shown in Fig. 8. The sampling frequency is 512Hz. The data is preprocessed to be of mean zero.

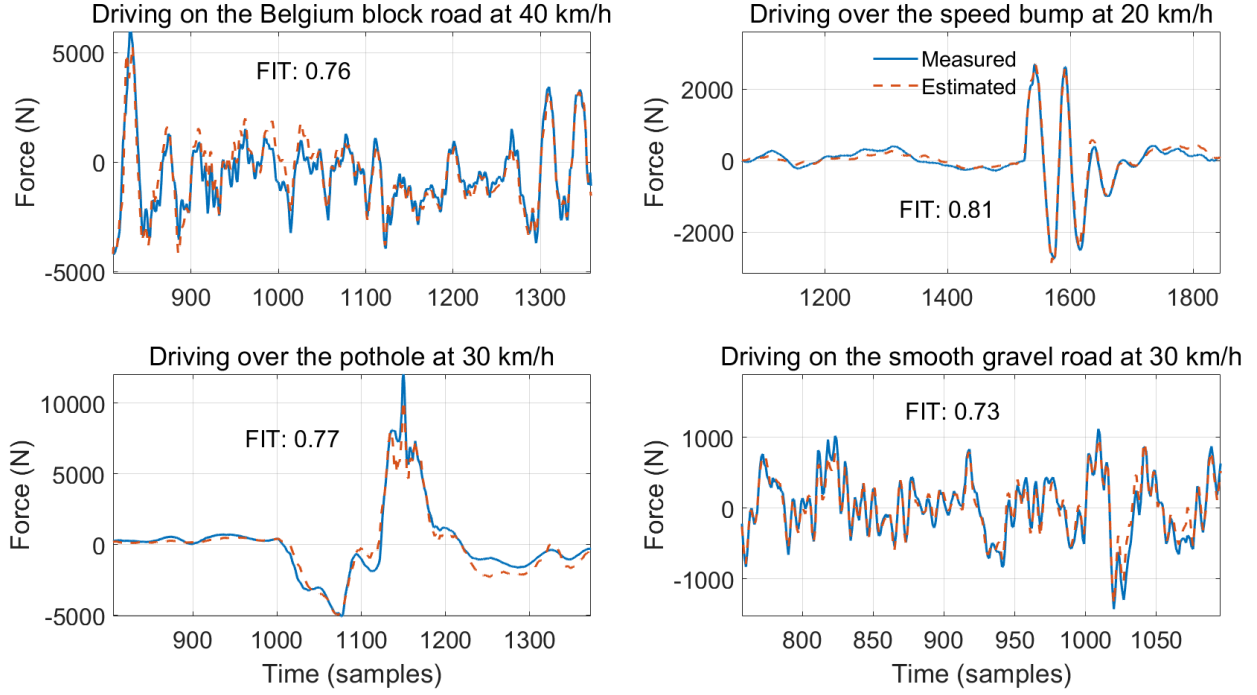


Figure 10: zoom in the result of Fig. 9 for the estimation performance on the four road profiles shown in Fig. 8. The sampling frequency is 512Hz. The data is preprocessed to be of mean zero.

Table 3: The estimation performances in the sense of FIT under 58 individual working conditions.

mean	standard deviation (std)	min	max	median
80.2%	5.6%	71.8%	90.8%	80.7%

5.2. An Illustrative Example of Primary-Auxiliary Model Scheduling Procedure for Estimation of the Vertical Wheel Force

In order to illustrate the primary-auxiliary model scheduling procedure presented in Section 3, five different working conditions are selected from the four categories shown in Tab. 2 (two from category one, each for one from remaining three categories) for constructing the transmissibility families \mathcal{H} and \mathcal{G} , and another three working conditions are used for the test during the online procedure. We set the prior distribution as $p(\mathbf{H}_q) = \frac{1}{5}$, $k = 1, \dots, 5$. As mentioned in Section 3, \mathbf{y}_I can be further decomposed into \mathbf{y}_{I_1} and y_{I_2} , with $\mathbf{y}_{I_1}(t) \in \mathbb{R}^{n_I-1}$ and $y_{I_2}(t) \in \mathbb{R}$ for each t . Following two principles in Remark 2, we denote by y_{I_2} the acceleration in X direction at position A in Fig. 7b, and \mathbf{y}_{I_1} the remaining accelerations and the suspension deflection.

Remark 3. From the physical insights, it is easily understood that the SNR of the acceleration in X direction is likely to be sufficient whenever the driver of the test vehicle is driving straight on a rough road, steering, or braking. Furthermore, in order to follow that the relation from \mathbf{y}_{I_2} to y_{I_1} has to be different under different offline working conditions (i.e., the second principle in Remark 2) as far as possible, the transmissibility families \mathcal{G} and \mathcal{H} are constructed from four different working condition categories shown in Tab. 2.

We may also verify that the acceleration in X direction at position A in Fig. 7b is suitable for serving as y_{I_2} in terms of Power Spectral Densities (PSD) signals in the frequency domain. Fig. 11 shows the PSD signals of the accelerations in X, Y, Z directions when the test vehicle is driven under four working conditions from different categories. For frequencies above 80 Hz, the SNRs of the three accelerations are not sufficient; For frequencies below 80 Hz, the SNRs of the three accelerations are sufficient under the first two working conditions (i.e., the vehicle is driven on Belgium block road or over speed bump). Particularly, a zoom in the same results when the driver of the test vehicle is braking or steering is shown in Fig 12, from which we observe that the SNRs of the acceleration in X direction are good at the low frequency range from 0 Hz to 5 Hz. On the contrary, the SNR of the acceleration in Y direction is poor when the driver is braking, which also conforms to the physical insights.

Fig. 13 shows good accordance between the measurement and the estimates from the scheduled estimator obtained by the proposed model scheduling procedure detailed in Section 3, which indicates the Bayes classifier successfully chooses an appropriate estimator under each online working condition.

Remark 4. An online working condition may or may not coincide with one from the offline working conditions for constructing the transmissibility families. Here we choose three online working conditions different from the previous five ones.

5.3. Estimation Under Multiple Online Working Conditions

Furthermore, we consider additional 53 online working conditions. A comparative study between the scheduled estimator and several other estimators is conducted in Subsection 5.3.1, and another comparative study between Bayes classifiers and a SVM classifier is conducted in Subsection 5.3.2.

5.3.1. A Comparative Study Between Several Estimators

Tab. 4 shows the performance of the scheduled estimator, individual estimators, an “average” estimator, as well as an “ideal” FIT (as a benchmark) in the aftermath under 53 online working

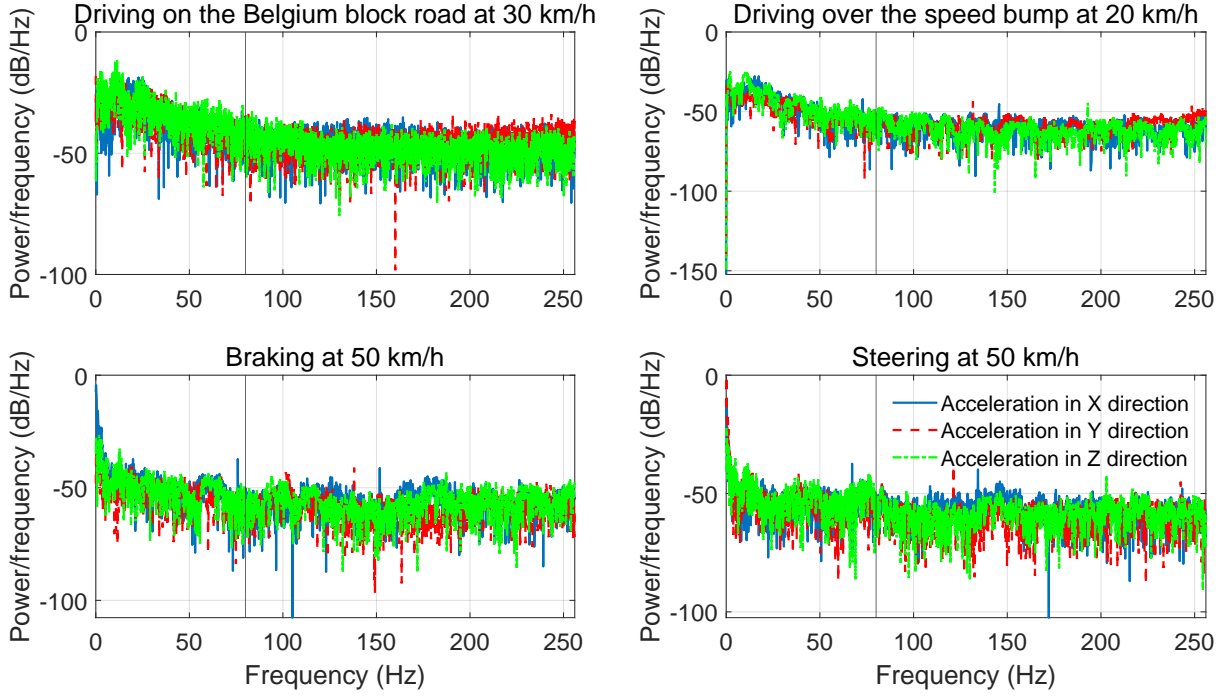


Figure 11: The PSDs of the accelerations in X, Y, Z direction at position A shown in Fig. 7b when the vehicle is driven under four typical working conditions. It can be observed that SNRs are not sufficient for frequencies above 80 Hz.

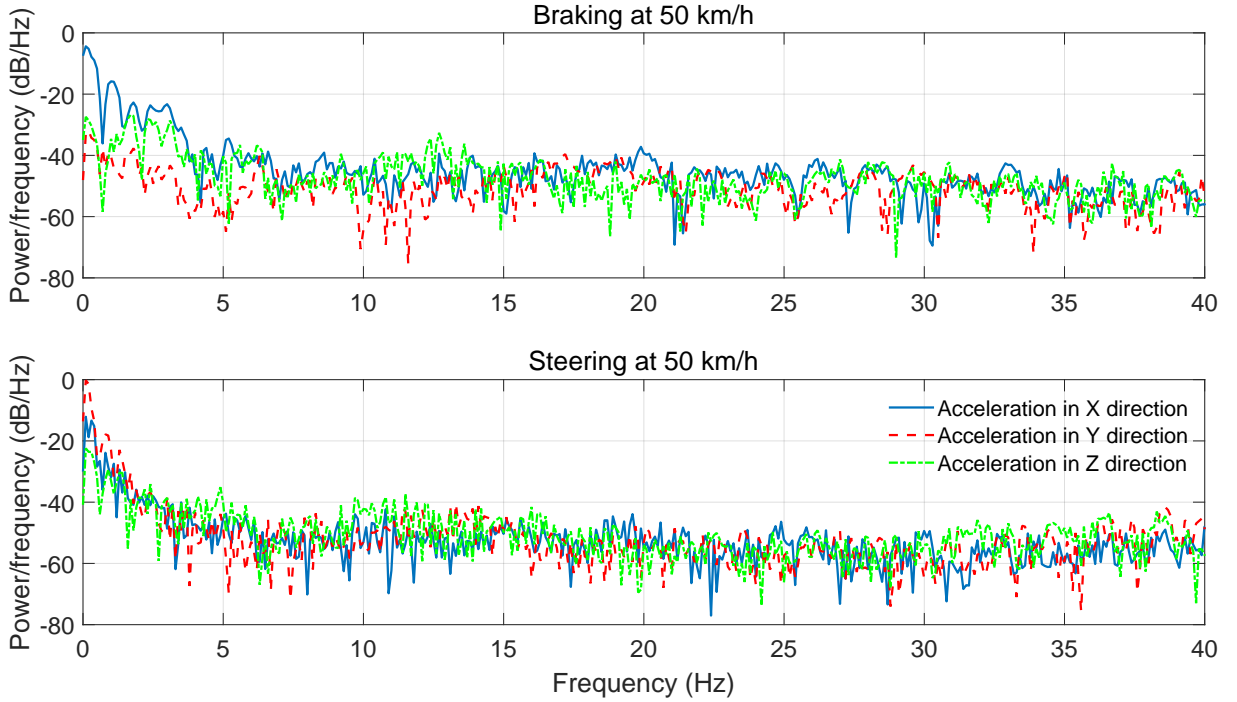


Figure 12: The zoom in the results of the PSDs of the accelerations in X, Y, Z direction under the braking and steering working conditions. It can be observed that the SNRs of the acceleration in X direction are good at low frequency range from 0 Hz to 5 Hz, while the SNR of the acceleration in Y direction is poor under the braking working condition.

conditions in the sense of mean and std of FIT calculated by Eq. (31). Note that the individual estimators are $\{\hat{y}_O(t)\}$ calculated from $\mathbf{G}_1, \dots, \mathbf{G}_5$. The “average” estimator is calculated by an “average” FIR model whose parameters are obtained by solving a single minimization problem with

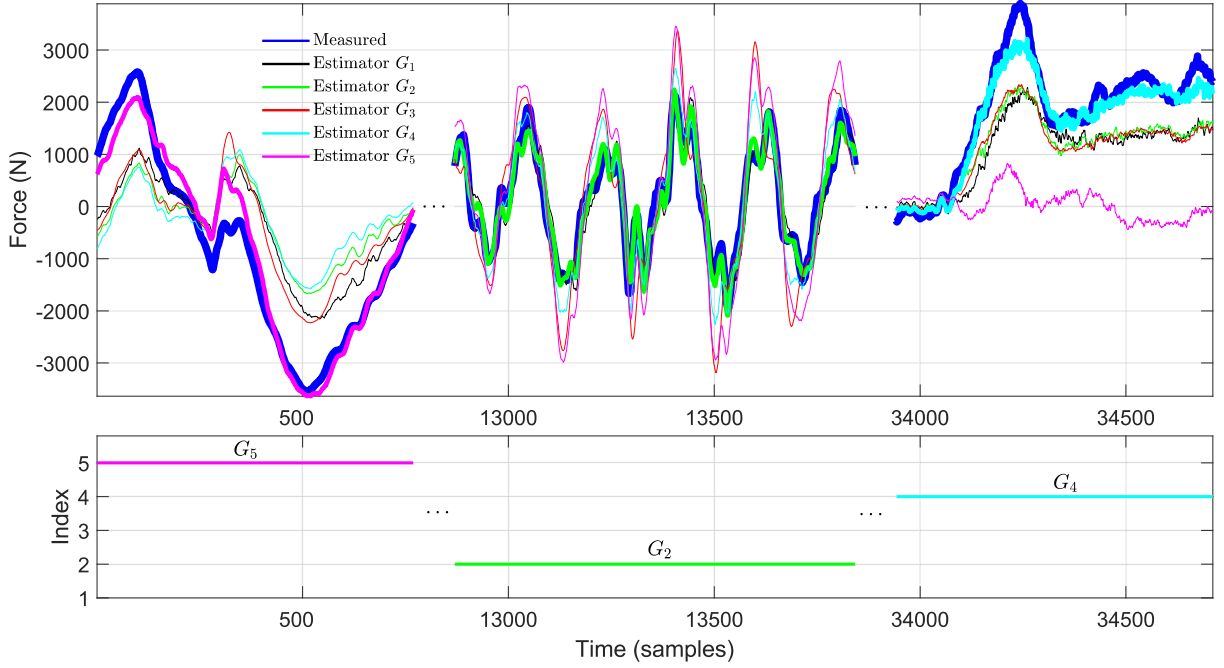


Figure 13: The primary-auxiliary model scheduling procedure. Top: the output y_O and estimates from \mathcal{G} . Bottom: evolution of primary transmissibilities. The sampling frequency is 512 Hz. The data is preprocessed to be of mean zero.

five offline working conditions putting together, i.e.,

$$\underset{\theta}{\text{minimize}} \quad \sum_{q=1}^5 \|\mathbf{Y}_O^q - \Phi_I^q \theta\|_2^2 + \rho \theta^T \theta, \quad (32)$$

where $\{\mathbf{Y}_O^q, \Phi_I^q\}$ is the data set from offline working condition \mathcal{C}_q . The scheduled estimator is the one obtained from the model scheduling procedure detailed in Section 3. The “ideal” FIT is calculated as

$$\text{FIT}_{\text{Ideal}}(\mathcal{C}_i) = \max_{q \in \{1, \dots, 5\}} \text{FIT}(q; \mathcal{C}_i), \quad i = 1, \dots, 53, \quad (33)$$

where $\text{FIT}(q; \mathcal{C}_i)$ denotes the measure of FIT for q -th estimator \mathbf{G}_q under i -th online working condition \mathcal{C}_i . Tab. 4 shows that the scheduled estimator already outperforms the individual estimators and the “average” estimator. Note that the mean and std of FIT corresponding to the scheduled estimator are close but not identical to those of the “ideal” FIT, since the Bayes classifier may sometimes choose a transmissibility from \mathcal{G} that is not optimal for the purpose of estimation (more discussions will be given in Remark 7). Additionally, the number of offline working conditions for constructing the scheduled estimator is limited, with more offline working conditions, the performance will be improved in the sense of FIT.

5.3.2. A Comparative Study Between Bayes classifiers and SVM classifiers

For i -th online working condition, where $i = 1, \dots, 53$, define an indicator function

$$I_i = \begin{cases} 1, & \text{if } q^* \in \arg \max_{q \in \mathcal{Q}} \text{FIT}(q; \mathcal{C}_i), \\ 0, & \text{otherwise,} \end{cases} \quad (34)$$

Table 4: Mean and std of FIT of the vertical force under 53 working conditions.

Estimators	mean (%)	std (%)
\mathbf{G}_1	67.1	11.1
\mathbf{G}_2	61.9	13.2
\mathbf{G}_3	27.2	29.7
\mathbf{G}_4	64.1	14.1
\mathbf{G}_5	41.9	17.7
“Average” estimator	67.0	10.8
Scheduled estimator	72.2	10.5
“Ideal” FIT ¹	73.5	9.5

¹ As a benchmark, cf., Eq. (33).

where q^* denotes the index of the selected \mathbf{G}_{q^*} by the Bayes classifier or the SVM classifier.

We also define \mathcal{A} as the classification accuracy in order to compare the performances of the Bayes classifier and the SVM classifier:

$$\mathcal{A} = \frac{1}{53} \sum_{i=1}^{53} I_i. \quad (35)$$

Tab. 5 shows the classification accuracies of the Bayes classifiers and the SVM classifier, from which we can see that the SVM classifier (the hyperparameters are optimized as far as possible) has the worst performance of classifying the online working conditions. Also, Tab. 5 shows the result of Bayes classifier with pooled variances. Note that “pooled variances” means the variances are identical for all \mathbf{H}_q ’s in \mathcal{H} , i.e., $\hat{\sigma}_{I,q}^2 = \hat{\sigma}^2$ in Eq. (24). We can see that the information of variances improves the classification accuracy significantly.

Remark 5. The key reason behind the success of the Bayes classifier in classifying the online working conditions is the strategic construction of the auxiliary transmissibility family \mathcal{H} such that one-to-one correspondence between H_q and working condition \mathcal{C}_q is constructed. Once the working condition is determined, the appropriate primary transmissibility G_q can be selected to estimate the unknown output.

Remark 6. The possible reason why the SVM classifier has the worst performance is that the dimension of the regressor domain is much higher than the one in piecewise affine ARX models (In the case study, for a seven input and one output MISO FIR model of order 50, the dimension of the regressor is 350) [21, 22]. Thus, classifying regressors directly with SVM classifiers might be problematic in sensor-to-sensor problems for the purpose of signal estimation, and more complicated classifiers with nonconvex optimization methods need to be involved, which increases the computational burden and makes the solution hard to assess.

Remark 7. The dynamics of the vehicle system under some online working conditions is possibly the same as or is quite close to the dynamics under corresponding offline working conditions, although the 53 online working conditions differ from the 5 offline working conditions. Thus, the proposed Bayes classifier can choose appropriate primary transmissibilities for estimating the unknown output under these online working conditions (under which the dynamics is the same or is quite close to the one under corresponding offline working conditions). On the contrary, the proposed Bayes classifier could be ineffective for the online working conditions under which the dynamics differs from the

Table 5: The classification accuracies of three classifiers.

	Bayes classifier	Bayes classifier (pooled variances)	SVM classifier
Accuracy	74%	64%	41%

one under 5 offline working conditions. Obviously, we can reduce the limitation by increasing the number of offline working conditions, which also increase the computational cost in real-time systems.

6. Conclusion and Future Works

In this work, a novel method is carried out to address signal estimation problems in nonlinear mechanical systems subject to non-stationary and unknown excitation by constructing pairs of transmissibility families: The system is treated as a switching linear system, where both the inputs and the working conditions are unknown. In addition to constructing a primary transmissibility family from the pseudo-inputs to the output, an auxiliary transmissibility family is constructed by decomposing the pseudo-input vector into two parts. The auxiliary family constructed from the pseudo-inputs enables to determine the unknown working condition (which is the bottleneck in the signal estimation problem) such that an appropriate transmissibility from the primary transmissibility family is selected for estimating the unknown output. Furthermore, the model order of FIRs, offline working conditions, and the outputs of auxiliary transmissibilities are selected in a sensible manner. As a result, the proposed approach offers a generalizable and explainable solution to the signal estimation problems in nonlinear mechanical systems in the context of switching linear dynamics with unknown inputs.

A real-world application to the estimation of the vertical wheel force in a full test vehicle is presented to demonstrate the effectiveness of the proposed method. In the illustrative example, good accordance between the measurement and the estimates from the proposed method is achieved. Also, the proposed method outperforms the competitive methods in the senses of FIT and the classification accuracy under multiple online working conditions.

The following challenge will be addressed in the future work: the success of proposed model scheduling method for the estimation of the vertical wheel force leads to the investigation of sufficient and necessary conditions under which the best primary transmissibility can be selected correctly according to the auxiliary transmissibility, which will further lead to the investigation of a theoretical framework of discrete mode observability [32] of switching linear systems with unknown inputs in transmissibility contexts.

References

- [1] P. Johannesson, M. Speckert, Guide to load analysis for durability in vehicle engineering, John Wiley & Sons, 2013.
- [2] M. El-kafafy, P. Csurscia, B. Cornelis, R. Enrico, K. Janssens, Machine learning and system identification for the estimation of data-driven models: an experimental case study illustrated on a tire-suspension system, in: Proceedings of the International Conference on Noise and Vibration Engineering (ISMA), KU Leuven, 2020, pp. 3287–3301.

- [3] E. Risaliti, T. Tamarozzi, M. Vermaut, B. Cornelis, W. Desmet, Multibody model based estimation of multiple loads and strain field on a vehicle suspension system, *Mechanical Systems and Signal Processing* 123 (2019) 1–25. doi:10.1016/j.ymssp.2018.12.024.
- [4] E. Risaliti, T. Tamarozzi, B. Cornelis, W. Desmet, Virtual sensing of wheel center loads on a mcpherson suspension, in: 28th International Conference on Noise and Vibration Engineering (ISMA2018), Leuven, Belgium, 2018, pp. 17–19.
- [5] W.-J. Yan, M.-Y. Zhao, Q. Sun, W.-X. Ren, Transmissibility-based system identification for structural health monitoring: Fundamentals, approaches, and applications, *Mechanical Systems and Signal Processing* 117 (2019) 453–482. doi:10.1016/j.ymssp.2018.06.053.
- [6] K. F. Aljanaideh, D. S. Bernstein, Experimental application of time-domain transmissibility identification to fault detection and localization in acoustic systems, *Journal of Vibration and Acoustics* 140 (2) (2018). doi:10.1115/1.4038436.
- [7] A. M. D’Amato, A. J. Brzezinski, M. S. Holzel, J. Ni, D. S. Bernstein, Sensor-only noncausal blind identification of pseudo transfer functions, *IFAC Proceedings Volumes* 42 (10) (2009) 1698–1703. doi:10.3182/20090706-3-FR-2004.00282.
- [8] A. J. Brzezinski, S. L. Kukreja, J. Ni, D. S. Bernstein, Identification of sensor-only mimo pseudo transfer functions, in: 2011 50th IEEE Conference on Decision and Control and European Control Conference, IEEE, 2011, pp. 2154–2159. doi:10.1109/CDC.2011.6160978.
- [9] K. F. Aljanaideh, D. S. Bernstein, Time-domain analysis of sensor-to-sensor transmissibility operators, *Automatica* 53 (2015) 312–319. doi:10.1016/j.automatica.2015.01.004.
- [10] J. Linder, M. Enqvist, Identification of systems with unknown inputs using indirect input measurements, *International Journal of Control* 90 (4) (2017) 729–745. doi:10.1080/00207179.2016.1222557.
- [11] C. Devriendt, G. De Sitter, P. Guillaume, An operational modal analysis approach based on parametrically identified multivariable transmissibilities, *Mechanical Systems and Signal Processing* 24 (5) (2010) 1250–1259. doi:10.1016/j.ymssp.2009.02.015.
- [12] S. Chesné, A. Deraemaeker, Damage localization using transmissibility functions: a critical review, *Mechanical systems and signal processing* 38 (2) (2013) 569–584. doi:10.1016/j.ymssp.2013.01.020.
- [13] A. RIBEIRO, J. SILVA, N. MAIA, On the generalisation of the transmissibility concept, *Mechanical Systems and Signal Processing* 14 (1) (2000) 29–35. doi:10.1006/mssp.1999.1268.
- [14] B. Peeters, G. De Roeck, Stochastic system identification for operational modal analysis: A review, *Journal of Dynamic Systems Measurement and Control-transactions of The Asme - J DYN SYST MEAS CONTR* 123 (12 2001). doi:10.1115/1.1410370.
- [15] W. Weijtjens, G. D. Sitter, C. Devriendt, P. Guillaume, Operational modal parameter estimation of mimo systems using transmissibility functions, *Automatica* 50 (2) (2014) 559 – 564. doi:10.1016/j.automatica.2013.11.021.

- [16] S. L. Kukreja, D. S. Bernstein, Sensor-only system identification for structural health monitoring of advanced aircraft, Tech. rep., NASA Armstrong Flight Research Center (2012).
- [17] L. Feng, X. Yi, D. Zhu, X. Xie, Y. Wang, Damage detection of metro tunnel structure through transmissibility function and cross correlation analysis using local excitation and measurement, *Mechanical Systems and Signal Processing* 60 (2015) 59–74. doi:10.1016/j.ymssp.2015.02.007.
- [18] A. J. Brzezinski, S. Kukreja, J. Ni, D. S. Bernstein, Sensor-only fault detection using pseudo transfer function identification, in: *Proceedings of the 2010 American Control Conference*, IEEE, 2010, pp. 5433–5438. doi:10.1109/acc.2010.5530787.
- [19] K. F. Aljanaideh, D. S. Bernstein, Time-domain analysis of motion transmissibilities in force-driven and displacement-driven structures, *Journal of Sound and Vibration* 347 (2015) 169–183. doi:10.1016/j.jsv.2015.01.018.
- [20] K. F. Aljanaideh, D. S. Bernstein, Output-only identification of input-output models, *Automatica* 113 (2020) 108686. doi:10.1016/j.automatica.2019.108686.
- [21] A. Garulli, S. Paoletti, A. Vicino, A survey on switched and piecewise affine system identification, *IFAC Proceedings Volumes* 45 (16) (2012) 344–355. doi:10.3182/20120711-3-be-2027.00332.
- [22] S. Paoletti, A. L. Juloski, G. Ferrari-Trecate, R. Vidal, Identification of hybrid systems a tutorial, *European journal of control* 13 (2-3) (2007) 242–260. doi:10.3166/ejc.13.242-260.
- [23] D. Liberzon, *Switching in systems and control*, Springer Science & Business Media, 2003.
- [24] L. Lennart, *System identification: theory for the user*, PTR Prentice Hall, Upper Saddle River, NJ (1999) 1–14.
- [25] M. S. Fledderjohn, M. S. Holzel, H. J. Palanthandalam-Madapusi, R. J. Fuentes, D. S. Bernstein, A comparison of least squares algorithms for estimating markov parameters, in: *Proceedings of the 2010 American Control Conference*, IEEE, 2010, pp. 3735–3740. doi:10.1109/acc.2010.5530673.
- [26] L. Ljung, T. Chen, What can regularization offer for estimation of dynamical systems?, in: *11th IFAC International Workshop on Adaptation and Learning in Control and Signal Processing (ALCOSP13)*, 3-5 July 2013, Caen, France, IFAC, 2013, pp. 1–8. doi:10.3182/20130703-3-fr-4038.00155.
- [27] J. R. Magnus, H. Neudecker, *Matrix differential calculus with applications in statistics and econometrics*, John Wiley & Sons, 2019.
- [28] T. Chen, L. Ljung, Implementation of algorithms for tuning parameters in regularized least squares problems in system identification, *Automatica* 49 (7) (2013) 2213–2220. doi:10.1016/j.automatica.2013.03.030.
- [29] C. M. Bishop, *Pattern recognition and machine learning*, Springer Science+ Business Media, 2006.

- [30] L. Ljung, System identification toolbox: User's guide, Citeseer, 1995.
- [31] A. Bemporad, A. Garulli, S. Paoletti, A. Vicino, A bounded-error approach to piecewise affine system identification, *IEEE Transactions on Automatic Control* 50 (10) (2005) 1567–1580. doi:10.1109/tac.2005.856667.
- [32] T. Boukhobza, Sensor location for discrete mode observability of switching linear systems with unknown inputs, *Automatica* 48 (7) (2012) 1262–1272. doi:10.1016/j.automatica.2012.05.011.